

CORROSION PERFORMANCE OF STEEL IN BLENDED CEMENT PORE SOLUTIONS

KOROZIJSKA ODPORNOST JEKLA V PORNIM VODAH IZ MEŠANIH CEMENTOV

Miha Hren^{1*}, Tadeja Kosec¹, Andraž Legat¹, Violeta Bokan-Bosiljkov²

¹Slovenian National Building and Civil Engineering Institute, Dimičeva ulica 12, 1000 Ljubljana, Slovenia

²Faculty of Civil and Geodetic Engineering, Jamova cesta 2, 1000 Ljubljana, Slovenia

Prejem rokopisa – received: 2019-01-03; sprejem za objavo – accepted for publication: 2019-04-04

doi:10.17222/mit.2019.003

Blended cements might change the chemistry of the pore solution and subsequently affect the corrosion of steel in concrete. Pore solutions were extracted, analyzed and compared from mortars made of CEM I, CEM II, CEM III and CEM IV cements. Three combinations of carbonation and chloride states were studied, i.e., non-carbonated without chlorides, non-carbonated with chlorides and carbonated with chlorides. Different electrochemical and spectroscopic techniques were used to study the electrochemical properties, the type and the extent of the corrosion products, as well as the type and the extent of the corrosion damage. It was confirmed that the most corrosive environments were pore solutions extracted from the carbonated mortars with chlorides. In this environment the highest corrosion rate was observed for the CEM III pore solution, and the lowest for the CEM I. The extent and the type of corrosion products and the corrosion damage varied according to the environment.

Keywords: corrosion, blended cements, pore solution, mortar

Cementi z mineralnimi dodatki lahko spremenijo strukturo porne vode in posledično vplivajo na korozijske lastnosti jekla. Porne vode so bile iztisnjene in analizirane iz malt, narejenih iz CEM I, CEM II, CEM III in CEM IV cementov. Malte so bile predhodno izpostavljene kloridom ali pospešeni karbonatizaciji v treh kombinacijah: brez karbonatizacije in brez kloridov, brez karbonatizacije s kloridi in v karbonatizaciji s kloridi. Za ugotavljanje korozijskih lastnosti jekla v pornih vodah so bile uporabljene različne elektrokemijske in spektroskopske metode. Analizirane so bile elektrokemijske lastnosti, tip in obseg korozijskih produktov ter tip in obseg korozijskih poškodb. Ugotovljeno je bilo, da najbolj korozivno okolje pripada pornim vodam v karbonatizirani malti s kloridi, kjer je bila najvišja korozijska hitrost izmerjena v pornih vodah iz CEM III cementa, najmanjša pa iz CEM I cementa. Obseg in tip korozijskih produktov ter poškodb se je razlikoval skladno s korozivnostjo okolja.

Ključne besede: korozija, mešani cementi, porna voda, malta

1 INTRODUCTION

The corrosion of rebar has been a longstanding durability issue in concrete. The penetration of the chloride ions and the reduction in the alkalinity due to carbonation can destabilize the passive film that protects the steel from corrosion. The use of certain mineral admixtures in blended cements affects both corrosion-propagation processes. These mineral admixtures primarily refine the concrete pores, which is a well-known beneficial effect that can slow down the chloride penetration and the carbonation progression.^{1,2} The same reactions that refine the pores also reduce the alkalinity³ and affect the chloride binding,⁴ thus creating a different and unknown corrosive environment.

Multiple corrosion studies have been conducted for mortars or concretes made of blended cements.^{5–14} Most of them focus on the additions of silica fume, fly ash and slag, with half-cell potential and linear polarization techniques being mostly used to determine the corrosion activity in the concrete or mortar. All the studies report on blended cements increasing the corrosion resistance due

to the latent pozzolanic reaction. However, not a lot of research focuses on aged concrete that has undergone carbonation, nor are there many examples of the corrosion rates being measured directly. There are many fewer corrosion studies available in concrete pore solutions extracted from blended cements. Most pore-solution experiments involved the use of saturated calcium hydroxide, with optional additions of potassium and sodium hydroxide.^{15–23} Electrochemical impedance spectroscopy and potentiodynamic polarization are the most common techniques used in these experiments. While chloride concentration and alkalinity are the two most important factors influencing steel corrosion, other ions found in the pore solution should not be overlooked.²⁴ So far, there is no information in the literature as to what extent the pore-solution's composition influences the corrosion of steel in blended cements.

In this paper the effect of the presence of chloride and carbonation was studied on the corrosion behavior of carbon steel in pore solutions extracted from mortars made of blended cements containing different amounts of fly ash, natural pozzolana and slag. Multiple electrochemical techniques, including corrosion-potential measurements, linear polarization and potentiodynamic

*Corresponding author's e-mail:
miha.hren@zag.si

scans, were used to study the corrosion properties. SEM, optical microscopy and Raman spectroscopy were employed to analyze the corrosion products formed in such media.

2 MATERIALS AND METHODS

Mortar prisms, 100 mm × 60 mm × 30 mm in size, were made to extract and analyze their pore solutions. Each prism had a water-cement ratio of 0.75 and a cement-aggregate ratio of 0.33. Standard sand, as described in EN 196-1:2016, was used and mixed with one of four different cements: CEM I 42.5 N, CEM II/B-M (LL-V) 42.5 N, CEM III/B (S) 32.5 N – LH/SR and CEM IV/A (V-P) 42.5 R SR. These cements differ in terms of the compressive strength and the admixtures used. Mineral admixtures are designated by the labels in parentheses, with some cements having multiple mineral admixtures. Label V is used for Fly ash, S is used for slag, LL is used for limestone and P is used for natural pozzolans. The cements were provided by a local cement factory, Salanit Anhovo.

All the specimens were cured for 28 d in a humidity chamber and one specimen of each cement also underwent accelerated carbonation for 10 w. These specimens are referred to in the text as carbonated, while the naturally carbonated specimens are referred to as non-carbonated. External chlorides were added through a 35-week cyclic ponding of 3.5 % sodium chloride solution, where the wetting period lasted for 3 d and the drying period lasted for 4 d. Reference specimens of each cement were also made to obtain pore water of uncarbonized mortars without external chlorides immediately after 28 d of curing in a humidity chamber.

The pore solution was extracted from the specimens using an extraction technique described in the literature.²⁵ A device was used that produces compressive pressure on the specimen in the range of 500 MPa to 1000 MPa and allowed the solution to be drained through a filter. A few ml of solution was extracted, diluted and analyzed using ion chromatography. Based on these results, a total of 12 synthetic pore solutions were prepared, where the cement type, chlorides and carbonation state were varied.

All the pore solutions were used as an electrolyte in 3 consecutive electrochemical experiments, with each set of tests repeated at least 3 times with a fresh working electrode and solution. The open-circuit potential (OCP) was measured first for about 22 h, until the potential of the working electrode stabilized. The linear polarization was measured at ±20 mV vs. OCP at a scan rate of 0.1 mV/s. The cyclic polarization followed from –250 mV vs OCP to 1.2 V above the reference potential, or until the current density reached 10 mA/cm². The scan rate was set at 1 mV/s. Tafel fitting was done in Gamry Echem Analyst software to obtain the corrosion potential, the corrosion-current density and both Tafel slopes.

In order to obtain the corrosion rates, the corrosion-current density was first calculated from the linear polarization using the Stern-Geary Equation (1). Anodic (β_a) and cathodic (β_c) Tafel slopes were acquired with the cyclic polarization. The corrosion rates were consecutively calculated from the corrosion-current density using Equation (2), where a is the atomic weight of iron (55.8 g/mol), n is the oxidation number of iron (2+) and ρ is the density of the steel (7.9 g/cm³).

$$i_{\text{corr}} = \frac{\beta_a \cdot \beta_c}{R_p \cdot 2.303(\beta_a + \beta_c)} \quad [\mu\text{m}/\text{cm}^2] \quad (1)$$

$$CR = 3.27 \frac{a \cdot i_{\text{corr}}}{n \cdot \rho} \quad [\mu\text{m}/\text{year}] \quad (2)$$

Electrochemical tests were done in Gamry Frameworks using the Gamry Reference 600 potentiostat. All the experiments were performed in a standard three-electrode cell, using a saturated calomel reference electrode (SCE), graphite counter electrode and a working electrode made of cold-rolled carbon-steel sheet with an exposed surface area of 1 cm². All the potentials in the text refer to the SCE potential. Prior to exposure, the steel surface was degreased with acetone and grinded using 600-grit, 1200-grit and 2500-grit papers. Immediately after the 24-hour electrochemical measurements, the electrodes were rinsed with distilled water, dried and examined under a Tagarno HD microscope. A low-vacuum JEOL 5500 LV SEM using an accelerating voltage of 20 kV and Horiba Yvon HR800 RAMAN spectrometer with a laser at $\lambda = 632$ nm and scanning range 50 cm⁻¹ to 1000 cm⁻¹ were also used to provide additional information about the surface of the steel and the corrosion products.

3 RESULTS AND DISCUSSION

3.1 Pore water extraction

The pore solutions were prepared according to the results of the mortar extraction (**Table 1**). Components were chosen so that the pH, chloride and sulfate concentrations (not shown) matched the values of the extracted

Table 1: Extracted pore solutions. Ion concentrations are in g/L

CEMENT	AC ¹	Cl ²	pH	Cl ⁻	[Cl ⁻]/[OH ⁻]
CEM I			13.06	0.07	0.017
		X	12.05	61.04	153
	X	X	10.45	82.83	8.29×10 ³
CEM II			13.03	0.10	0.026
		X	11.81	84.86	371
	X	X	7.52	106.37	9.06×10 ⁶
CEM III			12.51	0.40	0.349
		X	11.45	47.99	480
	X	X	7.54	117.08	9.53×10 ⁶
CEM IV			13.01	0.06	0.017
		X	12.06	74.91	184
	X	X	9.83	109.99	4.59×10 ⁴

1 – Accelerated Carbonation, 2 – External chlorides

solutions, while the cations were chosen to reflect the solutions as close as possible, due to solubility limitations. All the pH values were measured with a Mettler Toledo MP220 pH meter before and after exposure. They remained stable throughout the electrochemical experiments.

The pH of the untreated mortars, prepared by using different blended cements (CEM II, CEM III and CEM IV) and standard cement (CEM I) was as high as 13. The pore waters from the mortars that were exposed to cyclic ponding with chlorides contained around 48 g/L to 85 g/L chlorides and the pH was reduced to about 12, while the $[Cl^-]/[OH^-]$ ratio was between 150 and 480. The accelerated carbonation and cyclic wetting with chlorides resulted in a very high $[Cl^-]/[OH^-]$ ratio and a substantial decrease of the pH. Carbonation had the least effect on the CEM I pore solution's alkalinity (around pH 10), followed by CEM IV, CEM II and CEM III (around pH 7). The CEM III cement had the least amount of lime in its composition, which could be the reason for its lower alkalinity in all the exposed conditions (Table 1). All the cements showed a much higher chloride concentration after the accelerated carbonation. Although there are not many publications about carbonation and chloride binding, there seems to be a consensus that carbonation releases bound chlorides due to the reduction of pores for physical binding and the dissolution of Friedel's salt due to the lowered alkalinity.⁴ The latter would explain the higher concentration of chlorides in all the carbonated blended cements, especially CEM III. When naturally carbonated, CEM II had the largest amount of chlorides in its pore solution, followed by CEM IV, CEM I and CEM III. The chloride-binding capability of a cement is a combination of the alumina content, the C/S ratio, the level of carbonation, the sodium ions present and other factors.⁴ If one parameter does not stand out, a combination of all the factors influences the concentration of the bound chlorides. It is hard to determine to what degree each factor contributes to the chloride release.

3.2 Open-circuit potential

The open-circuit potential on steel in the pore solutions was measured for 22 h. In all the pore waters from the non-carbonated cement without chlorides, the potential increased over time, indicating that the high pH values made the steel more corrosion resistant compared to its in-air state. In some cases, the potential experienced more than a 100-mV drop after being stable for many hours. This may be due to the breakdown processes of the passive film formed in air, as a new, more stable passive film in alkaline solution forms. This process is known to take up to 3 d in alkaline solutions without aggressive ions.¹⁶ Similar trends are rarely observed for either non-carbonated or carbonated pore water with chlorides, as the potential decreased with time and remained relatively stable after a couple hours.

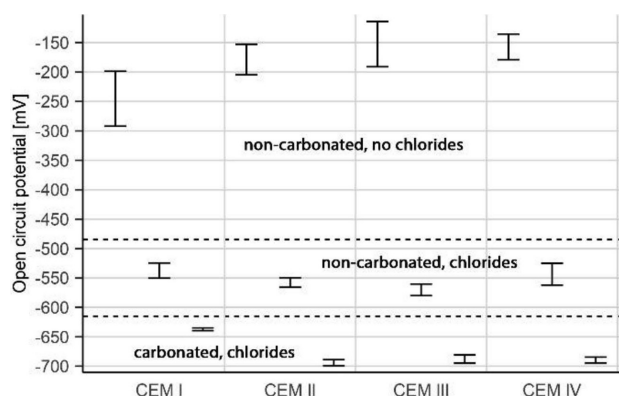


Figure 1: Open circuit potential values for all cements in all exposure states

The mean OCP error bar chart is shown in Figure 1 at the end of the exposure for pore waters of all 4 cements in the non-carbonated state without chlorides, the non-carbonated state with chlorides and the carbonated state with chlorides. Large differences were observed when comparing the corrosion potentials of the steel in cements in different chloride and carbonation states. The highest potentials were found in the non-carbonated pore water without chlorides, with a potential drop of around 350 mV observed for all the cements as the chlorides were added. The lowest potentials were measured in carbonated pore water with chlorides. These were between -700 mV and -620 mV.

The differences in the corrosion potentials of the steel in different cement types under the same mortar conditions were less expressed, but still differentiative. In the non-carbonated state without additional chlorides, the results cannot be correlated to either chloride concentrations or alkalinity. However, the highest concentrations of potassium, calcium, magnesium and sulfate ions can be found in the CEM I cement, which could explain its lower and less-stable potential.¹⁹ In the non-carbonated state with additional chlorides, the corrosion potential was the most positive for CEM I, followed by CEM IV and CEM II, while for CEM II it was the lowest (-570 mV). Results in the non-carbonated state with chlorides were in line with the $[Cl^-]/[OH^-]$ ratio (Table 1), where a higher ratio is reflected in a lower potential. In the carbonated pore solutions with chlorides, CEM I stood out with its lowest chloride content, highest pH and the resulting highest potential (-640 mV, Figure 1).

3.3 Polarization resistance

The results of the polarization resistance (R_p) measurements for 4 cements in 3 carbonation and chloride states are presented in Figure 2. The values of R_p are shown on a logarithmic scale. The polarization resistance is often translated to the corrosion rate through the Stern-Geary Equation (1) and Equation (2), where a higher polarization resistance results in a lower corrosion rate.

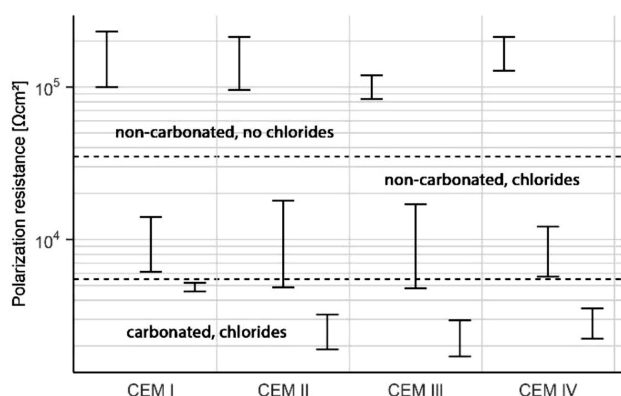


Figure 2: Polarization resistance values for all cements in all exposure states

Large differences in the polarization resistance can be seen between the different chloride and carbonation states. In the non-carbonated pore solution without chlorides, the polarization resistances were an order of magnitude higher for all the cements compared to R_p in the non-carbonated pore solution with chlorides. Thus, the corrosion rates in the non-carbonated pore solutions with chlorides were 10-times higher than for the steel in the non-carbonated pore solution without chlorides. The polarization resistance values between 1.5 $k\Omega\text{ cm}^2$ and 5 $k\Omega\text{ cm}^2$ in carbonated pore solutions with chlorides were 2.5-times lower than in the non-carbonated pore solutions with chlorides.

In the non-carbonated state without external chlorides, CEM III had a lower polarization resistance compared to the other cements, most likely due to the higher chloride concentration and the lower pH (Table 1). Almost no differences between the cements could be observed in the non-carbonated state with chlorides, apart from CEM II and CEM III having more scattered results. The performance of the cements in the carbonated state with chlorides was in line with the $[\text{Cl}^-]/[\text{OH}^-]$ ratio, where a higher ratio results in a lower resistance. The CEM III cement had the lowest polarization resistance, followed by CEM II, CEM IV and CEM I. In the carbonated state with chlorides, the steel in CEM I had the most positive R_p (5 $k\Omega\text{ cm}^2$).

3.4 Cyclic polarization

Potentiodynamic scans for the steel in pore solutions simulating the non-carbonated pore solution with and without chlorides and the carbonated pore solution with chlorides are presented in Figure 3. The corrosion-current density j_{corr} and the corrosion potential E_{corr} were deduced from the polarization curves and both are presented in Table 2. Using Equation (2), the corrosion rate v_{corr} was calculated from the j_{corr} values.

In the non-carbonized pore solution without chlorides, the polarization curves showed good corrosion resistance for the steel (Figure 3a). The corrosion potential was between -250 mV for CEM I and -130 mV for

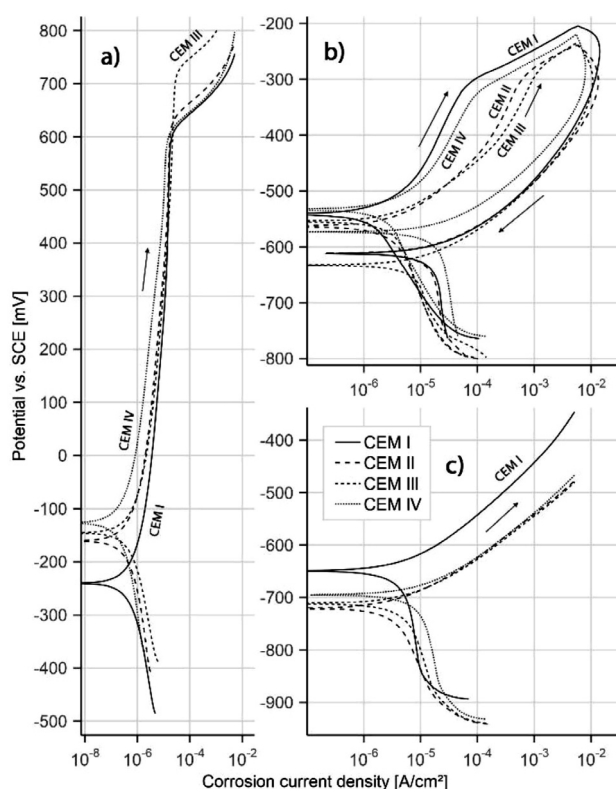


Figure 3: Cyclic polarization curves of select specimens in: a) non-carbonated pore water without chlorides, b) non-carbonated pore water with chlorides and c) carbonated pore water with chlorides

CEM IV. The corrosion-current densities were similar at 1 $\mu\text{A}/\text{cm}^2$, and the resulting corrosion rates did not exceed 20 $\mu\text{m}/\text{y}$ (Table 2). CEM IV showed the best corrosion resistance with both the lowest corrosion current and passive current densities (Figure 3a), followed by CEM I, CEM II and CEM III. The steel remained passive in all the pore solutions and the breakdown potential (E_b) was observed at roughly +600 mV vs. SCE, while E_b for CEM III was slightly more positive. During the reverse polarization cycle, the currents returned towards zero, following the same path as during anodic polarization. The shape of the potentiodynamic curves showed that no local type of corrosion is expected in such conditions.

In the non-carbonized pore solution with chlorides (Figure 3b), the corrosion potentials of the working electrodes were more negative due to the presence of chlorides. The values ranged between -650 mV and -500 mV. In terms of corrosion-current densities and the corresponding corrosion rates, CEM I, II, III and IV showed a similar average value of 3.5 $\mu\text{A}/\text{cm}^2$ (40 $\mu\text{m}/\text{y}$). The breakdown potential for all 4 cement pore solutions was reached at about -300 mV and the repassivation process required much lower potentials for the current density to reach values in the passive state. This is common for localized, chloride-induced corrosion. After the reverse polarization cycle, the potentials decreased by about 100 mV, on average.

Table 2: Corrosion potential, corrosion current and corrosion rate for all cements obtained from cyclic polarization

CEMENT		E_{corr} [mV]		j_{corr} [$\mu\text{A}/\text{cm}^2$]		v_{corr} [$\mu\text{m}/\text{y}$]	
non-carbonated no chlorides	CEM I	-250	± 50	1.0	± 0.5	11	± 5
	CEM II	-190	± 30	1.2	± 0.5	14	± 5
	CEM III	-160	± 40	1.7	± 0.3	19	± 4
	CEM IV	-170	± 20	0.8	± 0.3	9	± 3
non-carbonated chlorides	CEM I	-590	± 20	3.0	± 2.0	40	± 20
	CEM II	-580	± 20	4.0	± 1.0	40	± 20
	CEM III	-590	± 20	4.0	± 1.0	40	± 10
	CEM IV	-610	± 40	3.0	± 2.0	30	± 20
Carbonated chlorides	CEM I	-646	± 1	6.0	± 1.0	70	± 10
	CEM II	-719	± 9	9.0	± 5.0	100	± 50
	CEM III	-710	± 10	9.0	± 5.0	110	± 50
	CEM IV	-705	± 8	9.0	± 3.0	110	± 30

CEM IV and CEM I exhibited lower passive current densities compared to CEM II and CEM III (**Figure 3b**). These results correlate well with the $[\text{Cl}^-]/[\text{OH}^-]$ ratio, as both CEM II and CEM III have an about 2–3 times higher ratio compared to CEM I and CEM IV.

In carbonated pore water with chlorides, the steel underwent general corrosion. In the polarization curves (**Figure 3c**) this was indicated by a lack of a passive region as the current density was increasing with the potential in the anodic direction. The corrosion rate was the smallest for CEM I and the highest for CEM II and CEM III (**Figure 3c, Table 2**). The specimens made of pore water from CEM II, III and IV showed little difference in terms of the average current densities and corrosion rates (**Table 2**, values around $9 \mu\text{A}/\text{cm}^2$ and $100 \mu\text{m}/\text{y}$), with CEM IV having less-scattered results and a lower maximum expected corrosion rate as a result. The CEM I pore water stood out with a noticeably lower average and maximum expected corrosion rate ($70 \pm 10 \mu\text{m}/\text{y}$), which

is the result of its lower chloride content and higher alkalinity. Its corrosion potential was also higher by about 60 mV, in line with the OPC results. The optical microscopy and SEM images in **Figure 5a** and **5b** of the exposed working electrode in the carbonated pore solution with chlorides showed large areas of uniformly formed corrosion products. The size of the corroded area was larger when the pH was lower.

3.5 Optical microscopy, SEM and Raman

With the aim to follow the development of the corrosion products, the steel specimens were immersed in three different simulated environments (non-carbonated, non-carbonated with chlorides and carbonated with chlorides) of CEM I, CEM II, CEM III and CEM IV pore solutions. Only the steel specimens in the most corrosive CEM III environment are presented in **Figure 4**. The non-carbonated state (pH 12.54) of the CEM III pore solution was not aggressive and was observed to have no

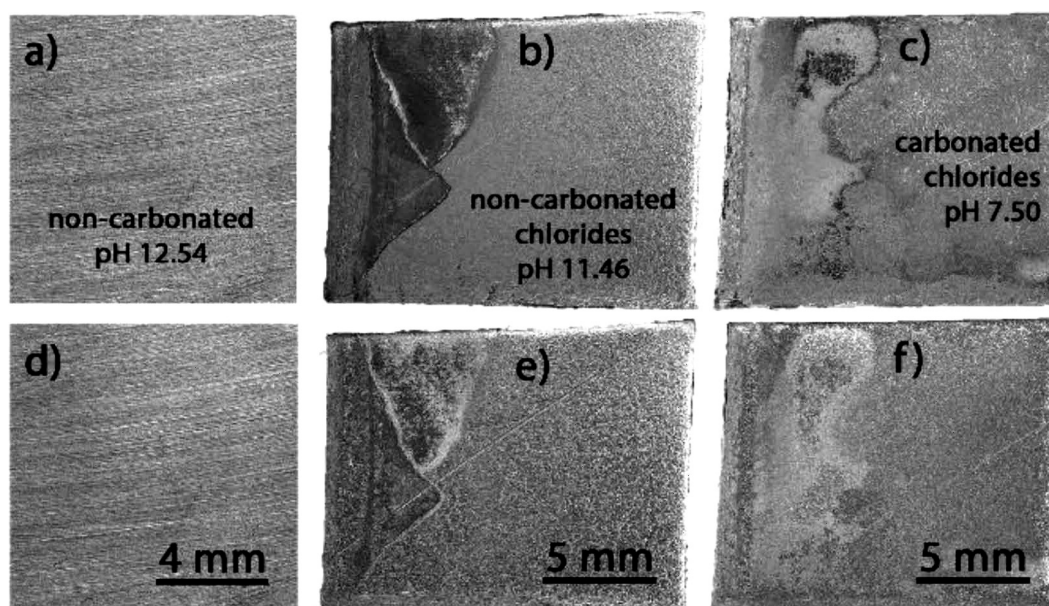


Figure 4: Photographs of steel specimen immersed in pore waters extracted from CEM III mortars exposed to different carbonation and chloride states: a) after 7 d, b) and c) after 18 d of exposure and d), e) and f) the same surfaces after cleaning of corrosion products in HCl with urotropine

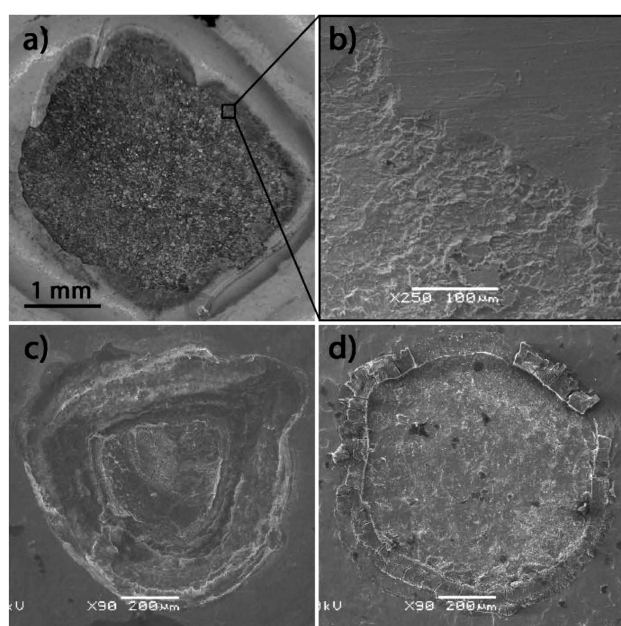


Figure 5: Optical and SEM images after 7 d of exposure: a) and b) steel surface in carbonated CEM III pore solution with chlorides, c) pit in non-carbonated CEM I pore solution with chlorides and d) pit in non-carbonated CEM II pore solution with chlorides

visible signs of corrosion (**Figure 4a**). In the non-carbonated state with chlorides (pH 11.46), the corrosion was already visible after 18 d of exposure (**Figure 4b**), where approximately one-third of the steel surface was covered in corrosion products. Almost the entire exposed surface of the steel was covered in corrosion products (**Figure 4c**) in the CEM III pore solution that was extracted from carbonated mortars soaked with chlorides (pH 7.50). The corrosion damage is shallow and not localized (**Figure 4e** and **4f**).

Optical microscopy and SEM were also used to examine the type of corrosion damage occurring on the specimens in each cement pore solution. No corrosion damage was detected on any of the specimens exposed to non-carbonated pore solutions without chlorides. In the non-carbonated pore solutions with chlorides, large isolated pits (CEM I and CEM II) and areas of localized corrosion along the edges of the specimen (CEM III and CEM IV) were detected. Two pits for CEM I and CEM II are shown in **Figure 5c** and **5d**, respectively. The extent and type of damage varied greatly between identical specimens in non-carbonated cements with chlorides, so no generalizations could be made. In the carbonated pore solutions with chlorides, general corrosion was observed for all the cements. Roughly 75 % and 35 % of the exposed area was corroded for the CEM I and CEM IV specimens, respectively. In the case of CEM II and CEM III, almost the entire exposed area was corroded (**Figure 5a**), which is in line with the lower pH values of these pore solutions.

SEM and Raman spectroscopy were used to study the morphology and the type of corrosion products present.

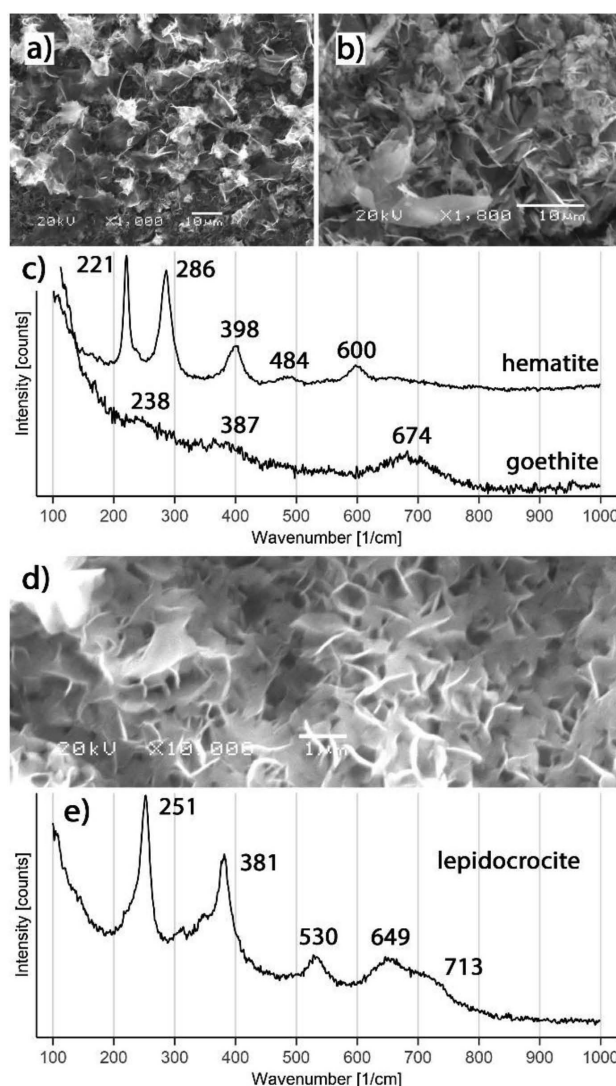


Figure 6: SEM images and Raman spectra of corrosion products found in: a), b) and c) non-carbonated CEM III pore solution with chlorides, d) and e) carbonated CEM III pore solution with chlorides

Similar corrosion products were found across multiple cements' pore solutions, so only the results from CEM III were evaluated in detail. The Raman spectra of the corrosion products formed on steel were compared to the Raman spectra reported in the literature.²⁶ On a specimen exposed to a non-carbonized pore solution with chlorides, strong hematite and weak goethite spectra were measured (**Figure 6a**, **6b** and **6c**). Hematite was characterized by two strong bands at 221 cm^{-1} and 286 cm^{-1} , one moderate band at 398 cm^{-1} and two weaker bands at 484 cm^{-1} and 600 cm^{-1} . The band around 240 cm^{-1} was not as pronounced as in the literature. Goethite showed a moderate band at 674 cm^{-1} and two very weak bands at 238 cm^{-1} and 387 cm^{-1} . Both the detected corrosion products are considered stable, adhere to the steel surface and slow down the corrosion reaction.¹⁸

The steel specimens in the carbonized pore solution with chlorides predominantly contained lepidocrocite on

their surface (**Figure 6d** and **6e**). Lepidocrocite was characterized by two strong bands at 251 cm^{-1} and 381 cm^{-1} , and three moderate bands at 530 cm^{-1} , 649 cm^{-1} and 713 cm^{-1} . Unlike goethite and hematite, this phase is unstable and porous.¹⁸ With time, it tends to dissolve and transform to other forms of oxides, thus offering weaker corrosion protection.

4 CONCLUSIONS

Pore waters were extracted from 4 cements exposed to a combination of carbonation and chlorides for 35 w. The following conclusions can be drawn.

Large differences in the corrosion rates, corrosion potentials, corrosion damage and corrosion products were observed when comparing different carbonation and chloride states of the pore solutions. The influence of these states on the corrosion conditions was significantly higher than that of the different cements.

When comparing different cement types (CEM I, CEM II, CEM III and CEM IV), it could be observed that the electrochemical properties varied, to some extent. However, these variations could be more significant when taking different degrees of corrosion localization into account.

In the non-carbonated state without chlorides the steel in the pore solution from all the cements showed passive behavior, with corrosion current densities as low as $1\text{ }\mu\text{A}/\text{cm}^2$. The post-exposure microscopic observations confirmed these results.

The corrosion damage in all the pore solutions from the carbonated cements with chlorides was roughly general, whereas the damage in the pore solutions from non-carbonated cements with chlorides was both localized and general.

Electrochemical techniques generally provided the lowest corrosion rates for CEM I, with the corrosion rates for CEM IV in non-carbonated conditions being somehow comparable to CEM I.

The highest corrosion rates overall were measured for CEM III. It should be mentioned, however, that the corrosion damage in both the carbonated and non-carbonated states with chlorides were roughly general.

Spectroscopic analyses of the corrosion products confirmed the electrochemical results. The Raman analysis indicated a protective corrosion layer in the non-carbonated chloride environment and non-protective corrosion products in the more corrosive carbonated chloride environment.

Acknowledgment

The financial support received from the Slovenian Research Agency (SRA) during 2015–2017, within the scope of the Young Scientist program, is hereby gratefully acknowledged.

5 REFERENCES

- P. K. Mehta, P. J. M. Monteiro, *Concrete: microstructure, properties, and materials*, McGraw-Hill, New York 2006, 660
- J. Bijen, Benefits of slag and fly ash, *Constr. Build. Mater.*, 10 (1996) 5, 309–314, doi:10.1016/0950-0618(95)00014-3
- A. Vollpracht, B. Lothenbach, R. Snellings, J. Haufe, The pore solution of blended cements: a review, *Mater. Struct.*, 49 (2016) 8, 3341–3367, doi:10.1617/s11527-015-0724-1
- Q. Yuan, C. Shi, G. De Schutter, K. Audenaert, D. Deng, Chloride binding of cement-based materials subjected to external chloride environment – A review, *Constr. Build. Mater.*, 23 (2009) 1, 1–13, doi:10.1016/j.conbuildmat.2008.02.004
- C. L. Page, N. R. Short, W. R. Holden, The influence of different cements on chloride-induced corrosion of reinforcing steel, *Cem. Concr. Res.*, 16 (1986) 1, 79–86, doi:10.1016/0008-8846(86)90071-2
- M. Maslehuddin, H. Saricimen, A. I Al-Mana, Effect of fly ash addition on the corrosion resisting characteristics of concrete, *ACI Mater. J.*, 84 (1987), 42-50
- P. S. Mangat, B. T. Molloy, Influence of PFA, slag and microsilica on chloride induced corrosion of reinforcement in concrete, *Cem. Concr. Res.*, 21 (1991) 5, 819–834, doi:10.1016/0008-8846(91)90177-J
- P. S. Mangat, J. M. Khatib, B. T. Molloy, Microstructure, chloride diffusion and reinforcement corrosion in blended cement paste and concrete, *Cem. Concr. Compos.*, 16 (1994) 2, 73–81, doi:10.1016/0958-9465(94)90002-7
- R. B. Polder, W. H. A. Peelen, Characterisation of chloride transport and reinforcement corrosion in concrete under cyclic wetting and drying by electrical resistivity, *Cem. Concr. Compos.*, 24 (2002) 5, 427–435, doi:10.1016/S0958-9465(01)00074-9
- V. Saraswathy, S. Muralidharan, K. Thangavel, S. Srinivasan, Influence of activated fly ash on corrosion-resistance and strength of concrete, *Cem. Concr. Compos.*, 25 (2003) 7, 673–680, doi:10.1016/S0958-9465(02)00068-9
- E. Güneysi, T. Özturan, M. Gesoğlu, A study on reinforcement corrosion and related properties of plain and blended cement concretes under different curing conditions, *Cem. Concr. Compos.*, 27 (2005) 4, 449–461, doi:10.1016/j.cemconcomp.2004.05.006
- M. A. Ibrahim, A. E.-D. M. Sharkawi, M. M. El-Attar, O. A. Hodhod, Assessing the corrosion performance for concrete mixtures made of blended cements, *Constr. Build. Mater.*, 168 (2018), 21–30, doi:10.1016/j.conbuildmat.2018.02.089
- N. Chousidis, I. Ioannou, E. Rakanta, C. Koutsodontis, G. Batis, Effect of fly ash chemical composition on the reinforcement corrosion, thermal diffusion and strength of blended cement concretes, *Constr. Build. Mater.*, 126 (2016), 86–97, doi:10.1016/j.conbuildmat.2016.09.024
- A. N. Borade, B. Kondraivendhan, Effect of metakaolin and slag blended cement on corrosion behaviour of concrete, *IOP Conf. Ser. Mater. Sci. Eng.*, 216 (2017) 1, 1-6, doi:10.1088/1757-899X/216/1/012022
- R. Liu, L. Jiang, J. Xu, C. Xiong, Z. Song, Influence of carbonation on chloride-induced reinforcement corrosion in simulated concrete pore solutions, *Constr. Build. Mater.*, 56 (2014), 16–20, doi:10.1016/j.conbuildmat.2014.01.030
- A. Poursaei, C. M. Hansson, Reinforcing steel passivation in mortar and pore solution, *Cem. Concr. Res.*, 37 (2007) 7, 1127–1133, doi:10.1016/j.cemconres.2007.04.005
- W. Chen, R.-G. Du, C.-Q. Ye, Y.-F. Zhu, C.-J. Lin, Study on the corrosion behavior of reinforcing steel in simulated concrete pore solutions using in situ Raman spectroscopy assisted by electrochemical techniques, *Electrochimica Acta.*, 55 (2010) 20, 5677–5682, doi:10.1016/j.electacta.2010.05.003
- J. K. Singh, D. D. N. Singh, The nature of rusts and corrosion characteristics of low alloy and plain carbon steels in three kinds of con-

- crete pore solution with salinity and different pH, *Corros. Sci.* 56 (2012) 129–142. doi:10.1016/j.corsci.2011.11.012.
- ¹⁹ P. Ghods, O. B. Isgor, G. McRae, T. Miller, The effect of concrete pore solution composition on the quality of passive oxide films on black steel reinforcement, *Cem. Concr. Compos.* 31 (2009) 2–11. doi:10.1016/j.cemconcomp.2008.10.003.
- ²⁰ M. Moreno, W. Morris, M. G. Alvarez, G. S. Duffó, Corrosion of reinforcing steel in simulated concrete pore solutions: Effect of carbonation and chloride content, *Corros. Sci.*, 46 (2004), 2681–2699, doi:10.1016/j.corsci.2004.03.013
- ²¹ F. Zhang, J. Pan, C. Lin, Localized corrosion behaviour of reinforcement steel in simulated concrete pore solution, *Corros. Sci.*, 51 (2009) 9, 2130–2138, doi:10.1016/j.corsci.2009.05.044
- ²² A. Česen, T. Kosec, A. Legat, V. Bokan-Bosiljkov, Corrosion properties of different forms of carbon steel in simulated concrete pore water, *Mater. Tehnol.*, 48 (2014) 1, 51–57
- ²³ G. Liu, Y. Zhang, Z. Ni, R. Huang, Corrosion behavior of steel submitted to chloride and sulphate ions in simulated concrete pore solution, *Constr. Build. Mater.*, 115 (2016), 1–5, doi:10.1016/j.conbuildmat.2016.03.213
- ²⁴ A. Poursaeed, C. M. Hansson, Potential pitfalls in assessing chloride-induced corrosion of steel in concrete, *Cem. Concr. Res.*, 39 (2009) 5, 391–400, doi:10.1016/j.cemconres.2009.01.015
- ²⁵ M. Cyr, P. Rivard, F. Labrecque, A. Daidić, High-pressure device for fluid extraction from porous materials: Application to cement-based materials, *J. Am. Ceram. Soc.*, 91 (2008) 8, 2653–2658, doi:10.1111/j.1551-2916.2008.02525.x
- ²⁶ F. Dubois, C. Mendibide, T. Pagnier, F. Perrard, C. Duret, Raman mapping of corrosion products formed onto spring steels during salt spray experiments. A correlation between the scale composition and the corrosion resistance, *Corros. Sci.*, 50 (2008) 12, 3401–3409, doi:10.1016/j.corsci.2008.09.027